Molecular BioSystems

Accepted Manuscript

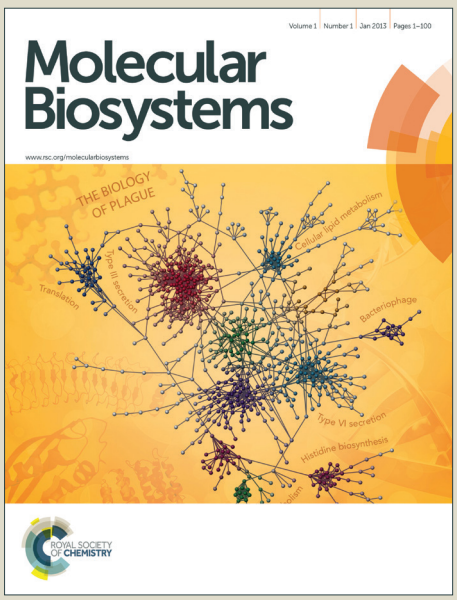

ROYAL SOCIETY OF CHEMISTRY

www.rsc.org/molecularbiosystems

Cite this: DOI: 10.1039/c0xx00000x

www.rsc.org/xxxxxx

ARTICLE TYPE

Features of S-Nitrosylation Based on Statistical Analysis and Molecular Dynamic Simulation: Cysteine Acidity, Surrounding Basicity, Steric Hindrance and Local Flexibility

Shangli Cheng,[a] Ting Shi,[a] Xiao-Lei Wang,[a] Liang Juan,[a] Hongyi Wu,[a] Lu Xie,[b] Yixue Li,[ab] and Yi-Lei Zhao*[ab]

Received (in XXX, XXX) Xth XXXXXXXXX 20XX, Accepted Xth XXXXXXXXX 20XX
DOI: 10.1039/b000000x

S-Nitrosylation involves in protein functional regulation and cellular signal transduction. Though intensive efforts were made, the molecular mechanisms of S-nitrosylation were not yet fully understood. In this work, we carried out a survey on 213 protein structures with S-nitrosylated cysteine sites and molecular dynamic simulations of hemoglobin as a case study. It was observed that the S-nitrosylated cysteines were of a lower pKa, a higher population of basic residues, a lower population of big-volume residues in the neighborhood, and higher flexibility, relatively. The case study of hemoglobin showed that, compared to that in the T-state, the Cysβ93 in the R-state hemoglobin possessed the above structural features, in agreement with the previous report that the R-state was more reactive in S-nitrosylation. Besides, basic residues moved closer to the Cysβ93 in the dep-R-state hemoglobin, while big-volume residues approached to the Cysβ93 in the dep-T-state. Using the four characteristics - cysteine acidity, surrounding basicity, steric hindrance, and local flexibility, a 3-dimensional model of S-nitrosylation was constructed to explain 61.9% of the S-nitrosylated and 58.1% of the non-S-nitrosylated cysteines. Our study suggests that cysteine deprotonation is prerequisite for protein S-nitrosylation, and these characteristics might be useful in identifying specificity of protein S-nitrosylation.

Introduction

Thiol group of cysteine is modified toward S-nitrosothiol in protein S-nitrosylation, and the process is reversible.[1,2] Accumulating evidences suggest that S-nitrosylation play a key role in regulation of protein functions,[3] human health and diseases[4,5] as well as cellular signaling.[6,7] In particular, protein S-nitrosylation is molecular basis of NO-related cellular signal transduction.[8,9] Many human diseases, such as Parkinson's disease,[10] neurodegeneration[11] and cancer,[8] even some physiological processes in plant[12] are related with S-nitrosylation. Biological methods and proteomic experiments are employed to identify the S-nitrosylated cysteine sites in proteins.[13-16]

It is reported that S-nitrosylation is highly specific and selective.[6,17] However, the mechanism of protein S-nitrosylation is still unclear.[18] Many possible pathways have been reported, such as 1) the NO depended S-nitrosylation,[18,19] 2) the trans-S-nitrosation,[20] 3) the Cu^{2+} induced S-nitrosylation in the presence of NO.[21] It is likely that deprotonation of thiol group of cysteine is involved in the pathways.[9,18] By using sequence-based bioinformatical method, the acid-based motif[22-24] and a revised acid-based motif[25] were proposed. Besides, structure-based analyses were reported as well.[25,26] For example, based on a few protein structures, S-nitrosylated cysteines were reported to have a higher predicted pKa values and locate in highly exposed areas of protein.[26] Up to now, few significant characteristics and rare systematic investigations were found on 3-demensional structures to explain the selectivity of S-nitrosylation.

A special case of S-nitrosylation is hemoglobin, in which the S-nitrosylation is preferentially formed on Cysβ93 in R-state hemoglobin, rather than T-state.[8] Conformational transition between R- and T-state hemoglobin, which is caused by oxygenation and deoxygenation, led to the S-nitrosylation and de-nitrosylation, respectively.[27-29] The Cysβ93 in the R-state hemoglobin is more reactive for S-nitrosylation than that in the T-state.[30] For the physiological significance, S-nitrosylation of hemoglobin can affect the response of hypoxic vasodilation in human respiratory cycle.[28] According to these reasons, hemoglobin is selected as a model protein to analyze the process of S-nitrosylation affected by structural changes, rather than sequence differences.

In our work, we collected 213 structures of S-nitrosylated proteins from PDB database by BLAST tool (Standard Protein BLAST in webserver of NCBI). The structure-based investigations on the S-nitrosylated proteins were carried out, including pKa, atomic distribution, steric hindrance and local

flexibility. Since the process of S-nitrosylation was related with the deprotonation of cysteine, the hemoglobin with deprotonated Cysβ93 was involved in this work. In all, four states of hemoglobin, including R-state, T-state, dep-R-state (R-state with deprotonated Cysβ93) and dep-T-state (T-state with deprotonated Cysβ93), were selected to detect dynamic characteristics. According to the discovered characteristics (Fig. 1), a 3-D structure-based S-nitrosylation model was constructed, explaining 61.92% of the S-nitrosylated and 58.13% of the non-S-nitrosylated cysteine sites in the collected proteins.

Materials and Methods

Collection of S-nitrosylated proteins

The S-nitrosylated proteins studied in this work were collected in sequence from the previously reported GPS-SNO paper[31] and references therein (Table S8, ESI†). The structural information of the S-nitrosylated proteins was then obtained by the BLAST tool and the PDB database. The BLAST thresholds of identity and positivity were set to be greater than 0.95. Overall 213 proteins containing 323 S-nitrosylated cysteine sites and 965 non-S-nitrosylated cysteine sites were obtained. In the redundancy analysis using CD-HIT,[32] sequence similarity of 179 S-nitrosylated proteins was less than 0.7. The CD-HIT was used to cluster and compare protein sequences by similarity tolerance.

Analysis of pKa

Acidity constant, pKa, can be the quantitative measurement of dissociation of thiol group (-SH). Because some PDB files contained the non-standard amino acids, they cannot be correctly recognized by the program of PROPKA 3.1,[33] in which the pKa value was estimated according to coulomb interactions, the description of internal and the surface residues. In our study, the pKa values of 276 out of S-nitrosylated cysteines and 685 out of non-S-nitrosylated cysteines were calculated based on protein structures by the program.

Analysis of neighboring atoms

The atoms of the neighboring residues were analyzed within a series of distant threshold, including 3.5, 4.0, 4.5, 5.0, 5.5, 6.0, 6.5, 7.0, 7.5 and 8.0 Å, where the distance was from the sulfur of all cysteine sites to the neighboring atoms. The 20 types of amino acids were grouped into five categories, i.e. polar amino acid (Ser, Thr, Cys, Pro, Asn, and Gln), acidic amino acid (Asp and Glu), basic amino acid (Lys, Arg, and His), aromatic amino acid (Phe, Tyr and Trp) and aliphatic amino acid (Gly, Ala, Val, Leu, Ile and Met).[34] Mann-Whitney test was used for the distributional analysis of the different types of atoms. The percentage difference value was defined in Formula 1.

Where PN(i), NN(i), P and N represent the number of atom(i) in S-nitrosylated set, the number of atom(i) in non-S-nitrosylated set, the number of S-nitrosylated cysteines and the number of non-S-nitrosylated cysteines, respectively. If the percentage difference value was greater than 0, the type of atoms was high abundant in S-nitrosylated cysteine set, and vice versa.

Analysis of steric hindrance

To analyze of the steric hindrance, the atoms (X) locating in front of the cysteine residues were selected, with the distance to the sulfur atom of cysteine less than 8 Å, and the angle of C-S---X larger than 90°, where the C atom was the side-chain carbon, and the X atom was located in the half ball of 8 Å (Fig. 4). The X atom could cause steric hindrance in the process of S-nitrosylation, which might prevent oxidant agents from attacking the thiol group.

Analysis of flexibility

The *B*-factor reflects the local structural fluctuations. In order to evaluate the local flexibility of S-nitrosylated or non-S-nitrosylated cysteine, the *B*-factor (*B*-value) of cysteine was calculated using Karplus algorithm by protein sequences.[35]

Hemoglobin and molecular dynamics simulations

Since the R- and T-state of hemoglobin shared the identical amino acid sequence with different capacity for S-nitrosylation,[36] the interactions between the neighboring amino acid residues and Cysβ93 site were investigated by molecular dynamics (MD) simulations based on four types of hemoglobins. The four types of hemoglobins included the R-state, T-state, dep-R-state and dep-T-state hemoglobins. The initial structures for R- and T-states of hemoglobin were chosen from 1HHO[37] and 2HHB[38] in PDB database. The full α2β2 structure of R-states were constructed with α and β subunits (1HHO) based on symmetry.[39]

In the preparation of four hemoglobin structures, histidine residues connecting to the heme were protonated at the δ-position, while the other histidine residues were protonated at the ε-position. The hemoglobin molecules were immersed in the octahedral boxes of TIP3P water with 10 Å to the edge. In all, the systems of R-state, T-state, dep-R-state and dep-T-state contained 8870, 8956, 8864 and 8955 water molecules, respectively. Six sodium ions in the cases of R-state and T-state[40] and eight sodium ions in the cases of dep-R-state and dep-T-state were added into the water boxes for charge neutralization. In the MD simulations, the AMBER force field 99SB was used for all amino acids and heme motif.[41] The cut-off of 10.0 Å[40] and SHAKE algorithm[42,43] were used for the short-range non-bonded and hydrogen bonds under periodic boundary condition. After the conjugate gradient method was performed under the minimization step, the system was gradually heated from 0 to 300 K. Finally, the 20 ns simulations of the R-, T-, dep-R- and dep-T-state hemoglobins were carried out in the absence of any restraint under conditions of 300 K, NTP and time-step of 2 fs. Each simulation was repeated for 14 times, with rearranged random number. For each state of hemoglobin, 280 ns MD simulations were carried out. In total, 1120 ns MD trajectory were obtained. Typically, the frames in a range of 5 to 20 ns in each trajectory were used for analysis.

Results and discussions

S-Nitrosylated cysteine has a lower pKa

In our work, the pKa values of thiol group in cysteine residue were calculated using PROPKA 3.1. The results showed that the pKa value of the S-nitrosylated cysteine (11.54±2.54, using 276 S-nitrosylated cysteine sites) was lower than that of the non-S-nitrosylated cysteine (11.95±2.75, using 685 non-S-nitrosylated cysteine sites) (Fig. 2a). Compared to P-T Doulias' study[26], our data set covered and expanded the S-nitrosylated cysteines in his work, where pKa of S-nitrosylated cysteines (10.0±2.10, using

142 S-nitrosylated cysteine sites) was higher than non-S-nitrosylated cysteines' (9.88±2.20, using 559 non-S-nitrosylated cysteine sites) using PROPKA 2.0. If the complete dataset was used, our results still stood for that the pKa values of S-nitrosylated (227 sites) and non-S-nitrosylated (638 sites) were calculated as 9.36±3.24 and 9.89±2.68, respectively. We speculated that a larger data set and updated software might be responsible for the differences.

Since the average pKa values of S-nitrosylated and non-S-nitrosylated cysteine were all larger than physiological pH, the cysteines existed mostly in the protonated state. However, the lower pKa of S-nitrosylated cysteines was suggested that the thiol group (-SH) of S-nitrosylated cysteine would be relatively more feasible to be deprotonated than the non-S-nitrosylated cysteines. Moreover, in the case of hemoglobin, the S-nitrosylation of both R- and T-state Cysβ93 were accelerated under a more basic environment in previous study.[30] Such a pKa (>7.0) does not grant the formation of thiol anion (RS^-) yet, so basic environment was necessary to enhance the process.

Basic residues around S-nitrosylated cysteines improve and stabilize the deprotonated cysteines

To analyze the physicochemical environments around the sulfur of cysteine, we extracted the characteristics of atomic distribution of the 323 S-nitrosylated and 965 non-S-nitrosylated sites. According to five groups of amino acids, namely polar (S, T, C, P, N and Q), acidic (D and E), basic (K, R and H), aromatic (F, Y and W) and aliphatic (G, A, V, L, I and M) group, the percentage difference values (PDVs)[44] between S-nitrosylated and non-S-nitrosylated cysteines were calculated (Fig. 2b, Table S6.1-6.10, ESI†). The PDVs of different types of atoms were tested using Mann-Whitney test (Table S1-S5, ESI†). Within a range of less than 6 Å around the sulfur of cysteines, the basic and acidic residues were of a high abundancy in S-nitrosylated cysteine sites. It was suggested that S-nitrosylated cysteines distributed in highly charged environments. This result was consistent with the previous study of -SNO group surrounded by charged residues,[45,46] that is, the basic residues were present highly frequently in the S-nitrosylated cysteine sites. Among the basic residues, histidine was abundant in S-nitrosylated cysteines within 5.0 Å ($P<0.05$, Table S6.1-6.4, ESI†). These results suggested that a basic environment could facilitate the process of cysteine deprotonation under physiological pH. Moreover, for the aromatic and aliphatic groups, Phe ($P<0.05$, Table S6.3-6.10, ESI†), Leu ($P<0.05$, Table S6.3-6.10, ESI†) and Tyr (Table S6.3-6.10, ESI†) were of high abundancy in the non-S-nitrosylated cysteines in a distance range between 4.5 and 8 Å. These results demonstrated that a non-polar environment would be disfavored for S-nitrosylation.

Correspondingly, the hemoglobin MD simulations showed that more basic residues surrounded Cysβ93 in the R- and dep-R-state hemoglobin. The average distance from sulfur of Cysβ93 to the neighboring atoms was calculated by the repeated trajectories of MD simulations. The neighboring basic residues, including Hisβ92, Hisβ143, Hisβ146, Lysβ95 and Lysβ144, were analyzed based on different radius around the sulfur atom of Cysβ93. When the distance was set as less than 6 Å, it was observed that basic residues, especially Hisβ92 and Lysβ144, were presented more frequently around Cysβ93 in R-state than that in T-state hemoglobin (Fig. 3a, 3b). When the Cysβ93 was deprotonated in dep-R-state, basic residues of Hisβ143 and Lysβ144 moved closer to the Cysβ93 (Fig. 3c) and additional hydrogen bonds were formed between N-H and thiol anion in certain frames (Fig S1, ESI†) while only Hisβ146 approached to the Cysβ93 in dep-T-state hemoglobin (Fig. 3d). Thus, the deprotonated Cysβ93 immersed in a more basic environment in the dep-R-state hemoglobin. This indicated that basic amino acid residues likely stabilized the deprotonated Cysβ93, which might be important in the process of S-nitrosylation.

Integrating the analysis of 323 S-nitrosylated cysteines (Fig. 2b) and MD simulations of hemoglobin (Fig. 3), we proposed that basic amino acids, especially histidine, were critical for the S-nitrosylated cysteines. It was suggested that the basic amino acids could form basic environment that could be contributive for the deprotonation of S-nitrosylated cysteines and the stabilization of deprotonated cysteines. In the collected S-nitrosylated proteins, 49 S-nitrosylated proteins with 53 S-nitrosylated cysteines were in line with this characteristic (Table S7, ESI†).

Steric hindrance inhibits S-nitrosylation

In order to evaluate the steric hindrance caused by the neighboring atoms around the sulfur of S-nitrosylated and non-S-nitrosylated cysteines, we analyzed distributional characteristics of the neighboring atoms in the half ball of 8 Å (Fig. 4). The S-nitrosylated cysteines had less neighboring atoms than the non-S-nitrosylated cysteines, for that the medians and interquartile ranges were estimated as 48 and 19 for the former, 50 and 12 for the latter, respectively. ($P<0.01$, with Mann-Whitney test. See Fig S2, ESI†) When the atoms were attributed to amino acid residues and ranked by the volume of amino acids, it was found that the atoms of amino acids with big volume, such as Tyr, Phe, Arg, and Lue, were more in non-S-nitrosylated cysteines than that in S-nitrosylated cysteines (Fig. 4). The steric hindrance caused by these big-volume residues would affect the attacking of oxidant agents and the binding of NO group. Also, the previous study reported that there were more exposing S-nitrosylated cysteines than non-S-nitrosylated cysteines in protein structure.[25] Our results suggested that steric hindrance could disadvantage for the process of S-nitrosylation.

For comparison, the similar statistical analyses were carried out on the hemoglobin trajectories of MD simulations. The neighboring aromatic and aliphatic residues with big volume, including Pheβ103, Tyrβ145, Leuβ91 and Leuβ141, were analyzed based on different cut-off radius around the sulfur of Cysβ93. For R-, T-, dep-R- and dep-T-state hemoglobin, MD simulations were repeated for 14 times. The average distances were calculated from sulfur of Cysβ93 to the neighboring atoms. The results showed that these big-volume residues were closer to the Cysβ93 in T-state hemoglobin than that in R-state hemoglobin, especially Tyrβ145 (Fig. 5a, 5b). When the Cysβ93 was deprotonated, the big-volume residues, including Pheβ103, Tyrβ145 and Leuβ141, moved away in dep-R-state hemoglobin. And these big-volume amino acids were not observed around the Cysβ93 within the radius of 6 Å in dep-R-state hemoglobin (Fig. 5c**)**. Compared to the dep-R-state hemoglobin, Tyrβ145 was closed to Cysβ93 in dep-T-state hemoglobin (Fig 5c, 5d).

Based on these analyses, we extracted the characteristic that few residues with big volume located around S-nitrosylated

cysteine sites in protein structures. This represented less steric hindrance occurred around S-nitrosylated cysteines. Combined with the mechanism of oxidant-mediated S-nitrosylation, the big-volume residues would prevent the oxidant from attacking cysteine. In summary, it was indicated that steric hindrance would inhibit protein S-nitrosylation. This result was in good agreement with another oxidant-mediated post-translational modification of tyrosine nitration.[44]

S-Nitrosylated cysteines are more flexible

The *B*-factor can reflect the cysteine's fluctuation, and it can be used to evaluate the flexibility of cysteine. The *B*-factor values of the S-nitrosylated and non-S-nitrosylated cysteines were calculated using Karplus algorithm. Our calculations indicated that the S-nitrosylated cysteines (Score was 0.965 ±0.036) were more flexible than the non-S-nitrosylated cysteines (Score was 0.958 ±0.035).

For hemoglobin, there were three cysteines, including Cysα104, Cysβ93 and Cysβ112. The Cysβ93 in R-state can be S-nitrosylated. The cysteines of Cysα104, Cysβ112 in R-state, as well as cysteines of Cysα104, Cysβ112 and Cysβ93 in T-state cannot be S-nitrosylated. Thus, these five cysteines were used as non-S-nitrosylated cysteines. In the MD simulations of hemoglobin, the results showed that the Cysβ93 in the R-state had a larger RMSF than other five cysteines in both R- and T-state hemoglobin (Table 1), suggesting that the S-nitrosylated Cysβ93 was more flexible. It was also found that there was a free space (26.25 $Å^3$) near the Cysβ93 in the R-state hemoglobin (Fig. S3, ESI†), which would allow the Cysβ93 to move freely. This indicated that the Cysβ93 in the R-state hemoglobin would have more opportunity to contact with oxidant agents.

Furthermore, the distribution of dihedral angles (SG-CB-CA-C) in the Cysβ93 of hemoglobin was obtained, where SG, CB, CA and C denoted the sulfur atom, the carbon of side chain, the alpha carbon and the carbon of main chain, respectively. The dihedral angles in the R-state hemoglobin were stabilized at ~0^o (Fig. 6a), while the dihedral angles in the T-state hemoglobin moved back and forth at ~120^o and ~240^o (Fig. 6b). Moreover, the dihedral angles of the Cysβ93 in the dep-R-state hemoglobin were much more fluctuated, which could adopt ~0^o, ~120^o and ~240^o, compared to that in the dep-T-state (Fig. 6c, 6d).

In brief, the S-nitrosylated cysteines were more flexible in protein structures. When cysteines were deprotonated, the dihedral angles of the S-nitrosylated cysteines were more active and conducive to the sulfur of the S-nitrosylated cysteines contacting with oxidants.

Less Cys residues locate around S-nitrosylated cysteines

By calculating the atomic distribution of sulfur atoms from neighboring cysteines, we found that the sulfur atoms of these residues were less available around the S-nitrosylated cysteines (Fig. 7). The previous study also showed a similar phenomenon that there were less other cysteines in the neighboring region.[24] Especially, when the distance was less than 3.5 Å (The disulfide bond length is about 2.05 Å), the frequency of sulfur atoms of Cys around S-nitrosylated cysteine sites was much lower than that around the non-S-nitrosylated (Table S6, ESI†). It was considered that these reductive cysteines would compete with the cysteines for oxidant agents in the process of S-nitrosylation.

Deprotonation of non-S-nitrosylated cysteines causes instability of protein structures

Besides the consistent characteristics found in both statistic and molecular simulations, the instability of hemoglobin were noted when the non-S-nitrosylated cysteine of Cysβ93 was deprotonated in the dep-T-state hemoglobin. Based on the results of MD simulations, which were repeated for 14 times, the root-mean-square deviation (RMSD) of each trajectory was analyzed to evaluate the structural changes in R-, T-, dep-R- and dep-T-state (Fig. S4, ESI†). To assess the rate of change in hemoglobin structure during MD simulations, the average differential coefficient of the RMSD of each trajectory was calculated, where a larger average differential coefficient meant larger change in protein structure. Thus, for each state of hemoglobin (R-, T-, dep-R-, and dep-T-state), there were 14 values of average differential coefficient. According to the distribution of the average differential coefficient, the structure of dep-T-state hemoglobin changed largely compared to the dep-R-, T- and R-state (Fig. 8), suggesting a protein structure would become unstable when a "non-S-nitrosylated" cysteine was deprotonated. Furthermore, RMSD of each amino acid residue was calculated, and amino acids with larger RMSF gathered at the loop between Aspβ79 and Glyβ83 (Fig S5, ESI†). It was proposed that the deprotonation of Cysβ93 might enhance the movement of the loop through allosteric regulation.

Discussion

In this work, we collected 213 S-nitrosylated proteins with structural information, containing 323 S-nitrosylated cysteine sites and 965 non-S-nitrosylated cysteine sites. First, compared to the non-S-nitrosylated cysteines, the S-nitrosylated cysteines had a lower pKa, a higher abundancy of basic residues, such as His and Lys, and a lower abundancy of aromatic and aliphatic residues, such as Phe, Tyr and Leu. The basic residues formed a basic environment around the S-nitrosylated cysteines in S-nitrosylated proteins, while the aromatic and aliphatic residues formed non-polar environment around the non-S-nitrosylated. It was suggested that basic environment could enhance the cysteines' deprotonation, which might be an important step in S-nitrosylation. Furthermore, in MD simulations of hemoglobin, the basic residues became closer to the deprotonated Cysβ93 in the dep-R-state hemoglobin, suggesting that basic environments formed by basic residues can further stabilize the deprotonated cysteines. Second, the S-nitrosylated cysteines had a lower population of big-volume residues, such as Phe, Tyr and Leu, in the half ball of 8 Å. In MD simulations of hemoglobin, Pheβ103 and Tyrβ145 moved away when the Cysβ93 was deprotonated in the dep-R-state hemoglobin, while Tyrβ145 was closed to Cysβ93 in dep-T-state hemoglobin. Based on the mechanism of oxidant-mediated S-nitrosylation, the big-volume residues would prevent oxidant agents from approaching to contact with the cysteine sites. This indicated that steric hindrance might make significant contributions to the process of S-nitrosylation. Third, by the analysis of *B*-factor, the S-nitrosylated cysteines were more flexible in structures. In MD simulations of hemoglobin, the Cysβ93 in the R-state hemoglobin had a higher RMSF than that in the T-state. It was speculated that the flexibility of cysteines could affect the S-nitrosylation as well. In particular, the proper

fluctuation of the SG-CB-CA-C conformation in dep-R-state allowed the Cysβ93 sulfur atom to contact NO reagent by chance. In addition, a low abundancy of the sulfur atoms of neighboring Cys was observed in S-nitrosylated cysteines.

As we know it that the conformation of hemoglobin was R-state in lung, while the hemoglobin was T-state in vein.[27] A probable process of S-nitrosylation was proposed in hemoglobin according to our analyses. First, under physiological pH, the basic residues would enhance the deprotonation of the Cysβ93 in R-state hemoglobin. Second, the basic residues moved closer to the deprotonated Cysβ93 and stabilized it. Third, the big-volume residues moved away from the deprotonated Cysβ93. Then, in coordination with high flexibility, the Cysβ93 was S-nitrosylated by adding NO group in lung. However, there were not these S-nitrosylated characteristics in T-state hemoglobin. Since the S-nitrosylation was reversible, NO was released from the T-state hemoglobin in vein. This was the blood flow regulation by S-nitrosylation.

In previous study, S. M. Marino proposed a revised acid-based motif and a structural model (covered 15 S-nitrosylated proteins).[24] In our work, we proposed a 3-dimensional model of S-nitrosylation associated with the distribution of amino acid residues in protein structures (Fig. 9). If there were more basic residues (including His and Lys) and less big-volume residues (including Phe, Tyr and Leu) around a cysteine, it would be easier for the cysteine to be S-nitrosylated. The reason was that a cysteine could be deprotonated and stabilized by the neighboring basic residues. The charged environment formed by basic residues was necessary for S-nitrosylation.[44] Furthermore, less big-volume residues, which located around cysteine sites in protein structures, would allow NO agent to access the target cysteines. This model might shed light on the deep comprehension in the process of S-nitrosylation.

In the model, there were two major conditions: I) atom number of basic amino acids (His and Lys) were non-zero in a distance less than 5 Å (The distance was from sulfur of cysteine to the neighboring atoms); II) atom number of big-volume residues (Phe, Tyr and Leu) were less than twenty two in a distance less than 8 Å (twenty two was the average number of big-volume atoms in data set). Besides the two main conditions, a minor condition from statistical analysis (Fig 7, Table S1, ESI†) was extracted: III) no other cysteines existed in a distance less than 5 Å. Under these three conditions, the 3-D S-nitrosylation model explained 200 out of 323 S-nitrosylated cysteine sites (61.92%) and 561 out of 965 non-S-nitrosylated cysteine sites (58.13%).

Conclusion

In this work, 213 protein structures with 323 S-nitrosylated cysteine sites and 965 non-S-nitrosylated cysteine sites were collected to study characteristics of S-nitrosylation using statistical analyses and MD simulations, where hemoglobin was employed as a case. Four major characteristics were observed, including 1) a lower pKa, 2) a higher population of basic residues, 3) a lower population of big-volume residues in the neighborhood, and 4) higher flexibility. The MD simulations of hemoglobin showed that basic residues could enhance the deprotonation of S-nitrosylated cysteines, and the basic environments could further stabilize the deprotonated cysteines. Moreover, steric hindrance caused by big-volume residues would play important role in the process of S-nitrosylation, and the flexibility of cysteines could also affect the S-nitrosylation. In conclusion, a 3-dimensional model of S-nitrosylation was proposed, which could explain 61.9% of the S-nitrosylated and 58.1% of the non-S-nitrosylated cysteines. Our study suggested that deprotonation was a prerequisite for protein S-nitrosylation, and the model would improve the understanding of S-nitrosylation in structural characteristics. Much more structural characteristics based on larger dataset obtained by homology modeling would lead a more powerful structural model.

Acknowledgements

YLZ, LX, and YXL conceived and designed the investigation. SLC, JL, and HYW performed the structure analyses and MD simulations. SLC, TS, XLW, and YLZ wrote the paper. This work is supported in part by National High-Tech R&D Program of China “863” (No. 2012AA020403) and the National Basic Research Program of China “973” (Nos. 2012CB721005, 2013CB966802), National Science Foundation of China (Nos. 21377085, 21303101, 31121064, J1210047), MOE New Century Excellent Talents in University (No. NCET-12-0354), and the SJTU-HPC computing facility award.

Notes and references

[a] *State Key Laboratory of Microbial Metabolism, School of Life Sciences and Biotechnology, Shanghai Jiao Tong University, Shanghai 200240, China. Fax: +86-21-34207190; Tel: +86-21-34207190; E-mail: yileizhao@sjtu.edu.cn*

[b] *Shanghai Center for Bioinformation Technology, Shanghai 201203, China.*

1 D. T. Hess, A. Matsumoto, S. O. Kim, H. E. Marshall and J. S. Stamler, *Nat Rev Mol Cell Bio*, 2005, **6**, 150-166.
2 M. Benhar, M. T. Forrester and J. S. Stamler, *Nat Rev Mol Cell Bio*, 2009, **10**, 721-732.
3 Y. Iwakiri, *Nitric Oxide-Biol Ch*, 2011, **25**, 95-101.
4 M. W. Foster, T. J. McMahon and J. S. Stamler, *Trends Mol Med*, 2003, **9**, 160-168.
5 A. M. Evangelista, M. J. Kohr and E. Murphy, *Antioxid Redox Signal*, 2013, **19**, 1209-1219.
6 S. R. Tannenbaum and J. E. Kim, *Nat Chem Biol*, 2005, **1**, 126-127.
7 S. R. Jaffrey, H. Erdjument-Bromage, C. D. Ferris, P. Tempst and S. H. Snyder, *Nat Cell Biol*, 2001, **3**, 193-197.
8 Z. Q. Wang, *Cancer Lett*, 2012, **320**, 123-129.
9 D. D. Thomas and D. Jourd'heuil, *Antioxid Redox Signal*, 2012, **17**, 934-936.
10 J. G. Fang, T. Nakamura, D. H. Cho, Z. Z. Gu and S. A. Lipton, *P Natl Acad Sci USA*, 2007, **104**, 18742-18747.
11 D. H. Cho, T. Nakamura, J. G. Fang, P. Cieplak, A. Godzik, Z. Gu and S. A. Lipton, *Science*, 2009, **324**, 102-105.
12 C. Lindermayr and J. Durner, *J Proteomics*, 2009, **73**, 1-9.
13 H. Li, X. Xing, G. Ding, Q. Li, C. Wang, L. Xie, R. Zeng and Y. Li, *Mol. Cell. Proteomics*, 2009, **8**, 1839-1849.
14 G. Hao, B. Derakhshan, L. Shi, F. Campagne and S. S. Gross, *P Natl Acad Sci USA*, 2006, **103**, 1012-1017.
15 F. Torta, V. Usuelli, A. Malgaroli and A. Bachi, *Proteomics*, 2008, **8**, 4484-4494.
16 B. Derakhshan, P. C. Wille and S. S. Gross, *Nat Protoc*, 2007, **2**, 1685-1691.
17 D. A. Mitchell and M. A. Marletta, *Nat Chem Biol*, 2005, **1**, 154-158.
18 K. A. Broniowska, *Antioxid Redox Signal*, 2012, **17**, 969.
19 G. Czapski and S. Goldstein, *Free Radic Biol Med*, 1995, **19**, 785-794.

20 Y. Yang and J. Loscalzo, *P Natl Acad Sci USA*, 2005, **102**, 117-122.
21 G. Stubauer, A. Giuffre and P. Sarti, *J Biol Chem*, 1999, **274**, 28128-28133.
22 Y. J. Chen, W. C. Ku, P. Y. Lin, H. C. Chou, K. H. Khoo and Y. J. Chen, *J Proteome Res*, 2010, **9**, 6417-6439.
23 A. Martinez-Ruiz, L. Villanueva, C. Gonzalez de Orduna, D. Lopez-Ferrer, M. A. Higueras, C. Tarin, I. Rodriguez-Crespo, J. Vazquez and S. Lamas, *P Natl Acad Sci USA*, 2005, **102**, 8525-8530.
24 Y. Xu, J. Ding, L. Y. Wu and K. C. Chou, *PLoS One*, 2013, **8**, e55844.
25 S. M. Marino and V. N. Gladyshev, *J Mol Biol*, 2010, **395**, 844-859.
26 P. T. Doulias, J. L. Greene, T. M. Greco, M. Tenopoulou, S. H. Seeholzer, R. L. Dunbrack and H. Ischiropoulos, *P Natl Acad Sci USA*, 2010, **107**, 16958-16963.
27 T. J. McMahon, *Nat Med*, 2002, **8**, 711-717.
28 J. S. Stamler, L. Jia, J. P. Eu, T. J. McMahon, I. T. Demchenko, J. Bonaventura, K. Gernert and C. A. Piantadosi, *Science*, 1997, **276**, 2034-2037.
29 J. P. Pezacki, N. J. Ship and R. Kluger, *J Am Chem Soc*, 2001, **123**, 4615-4616.
30 L. Jia, C. Bonaventura, J. Bonaventura and J. S. Stamler, *Nature*, 1996, **380**, 221-226.
31 Y. Xue, Z. X. Liu, X. J. Gao, C. J. Jin, L. P. Wen, X. B. Yao and J. A. Ren, *PLoS One*, 2010, **5**, e11290.
32 Li, W. and A. Godzik, *Bioinformatics*, 2006. **22**, 1658-1659.
33 M. H. M. Olsson, C. R. Sondergaard, M. Rostkowski and J. H. Jensen, *J Chem Theory Comput*, 2011, **7**, 525-537.
34 T.-Y. Lee, Y.-J. Chen, T.-C. Lu, H.-D. Huang and Y.-J. Chen, *PLoS One*, 2011, **6**, e21849.
35 P. Karplus and G. Schulz, *Naturwissenschaften*, 1985, **72**, 212-213.
36 D. J. Singel and J. S. Stamler, *Annu Rev Physiol*, 2005, **67**, 99-145.
37 B. Shaanan, *J Mol Biol*, 1983, **171**, 31.
38 G. Fermi, *J Mol Biol*, 1984, **175**, 159.
39 L. Mouawad, D. Perahia, C. H. Robert and C. Guilbert, *Biophys J*, 2002, **82**, 3224-3245.
40 O. K. Yusuff, J. O. Babalola, G. Bussi and S. Raugei, *J Phys Chem B*, 2012, **116**, 11004-11009.
41 V. Hornak, R. Abel, A. Okur, B. Strockbine, A. Roitberg and C. Simmerling, *Proteins-Struct Funct Bioinform*, 2006, **65**, 712-725.
42 J. P. Ryckaert, *J. Comput. Phys.*, 1977, **23**, 327.
43 R. Gnanasekaran, Y. Xu and D. M. Leitner, *J Phys Chem B*, 2010, **114**, 16989-16996.
44 S. Cheng, B. Lian, J. Liang, T. Shi, L. Xie and Y. L. Zhao, *Mol Biosyst*, 2013, **9**, 2860-2868.
45 M. R. Talipov and Q. K. Timerghazin, *J Phys Chem B*, 2013, **117**, 1827-1837.
46 N. Gould, P. T. Doulias, M. Tenopoulou, K. Raju and H. Ischiropoulos, *J Biol Chem*, 2013, **288**, 26473-26479.

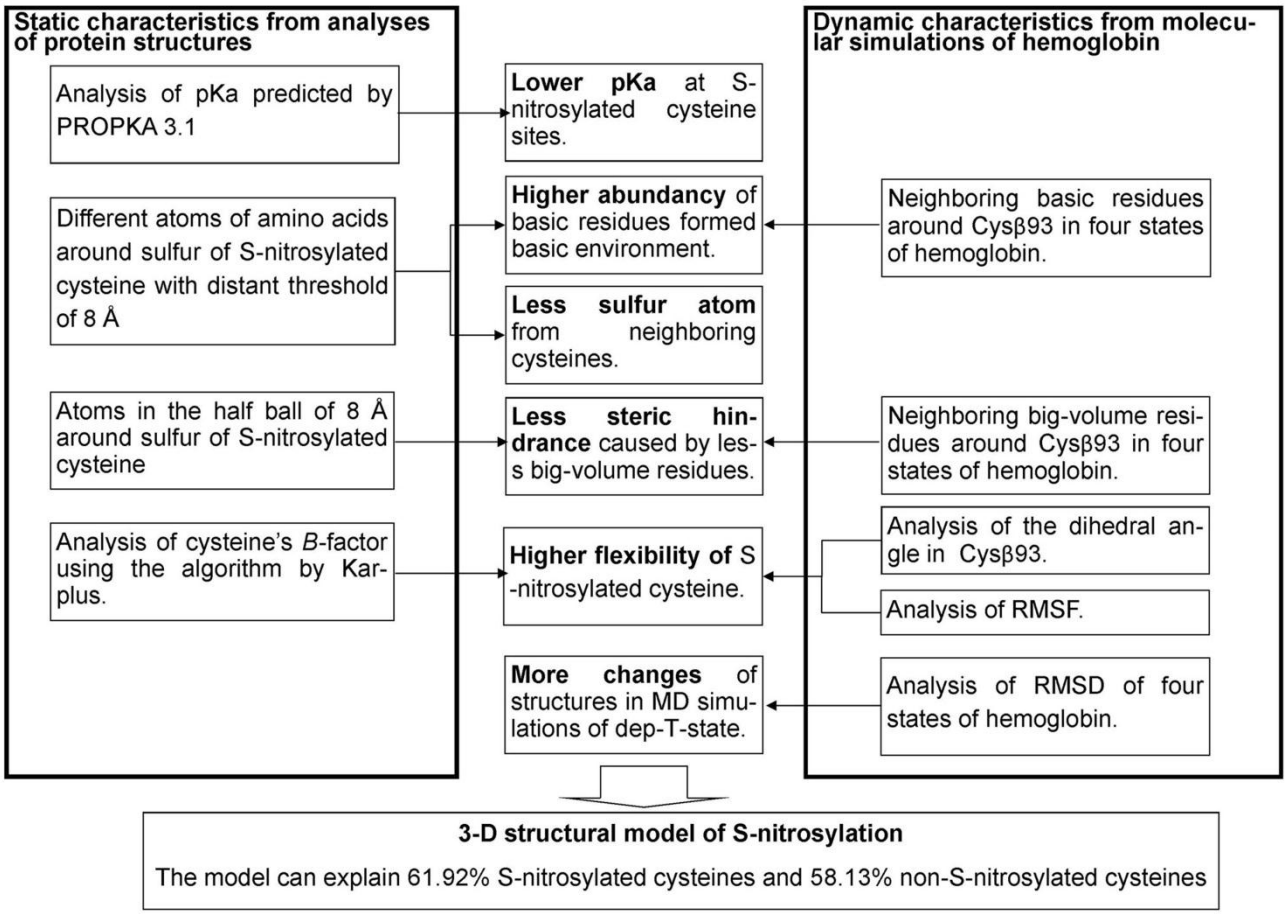

Fig. 1 The flow chart shows the correlations between S-nitrosylation and the characteristics.

5

Cite this: DOI: 10.1039/c0xx00000x

www.rsc.org/xxxxxx

ARTICLE TYPE

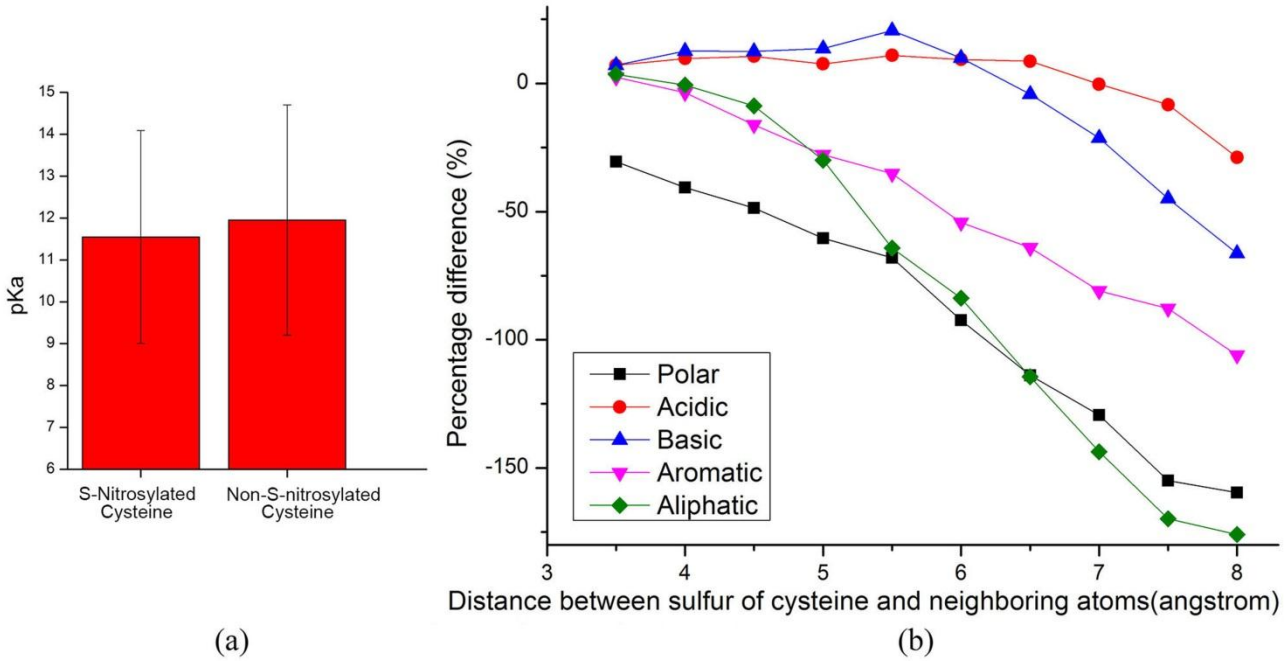

Fig. 2 The pKa of S-nitrosylated and non-S-nitrosylated cysteines, and the atomic distribution around the sulfur of S-nitrosylated cysteines. (a) The pKa of S-nitrosylated and non-S-nitrosylated cysteines was calculated using PROPKA 3.1. The y-axis represents the value of pKa. (b) The x-axis represents the distance (3.5 to 8.0 Å) from the sulfur of cysteine to the neighboring atoms. The y-axis represents the percentage difference values between the S-nitrosylated and non-S-nitrosylated cysteine sets. The Mann–Whitney test was used (Table S1-S5, ESI†).

Cite this: DOI: 10.1039/c0xx00000x

www.rsc.org/xxxxxx

ARTICLE TYPE

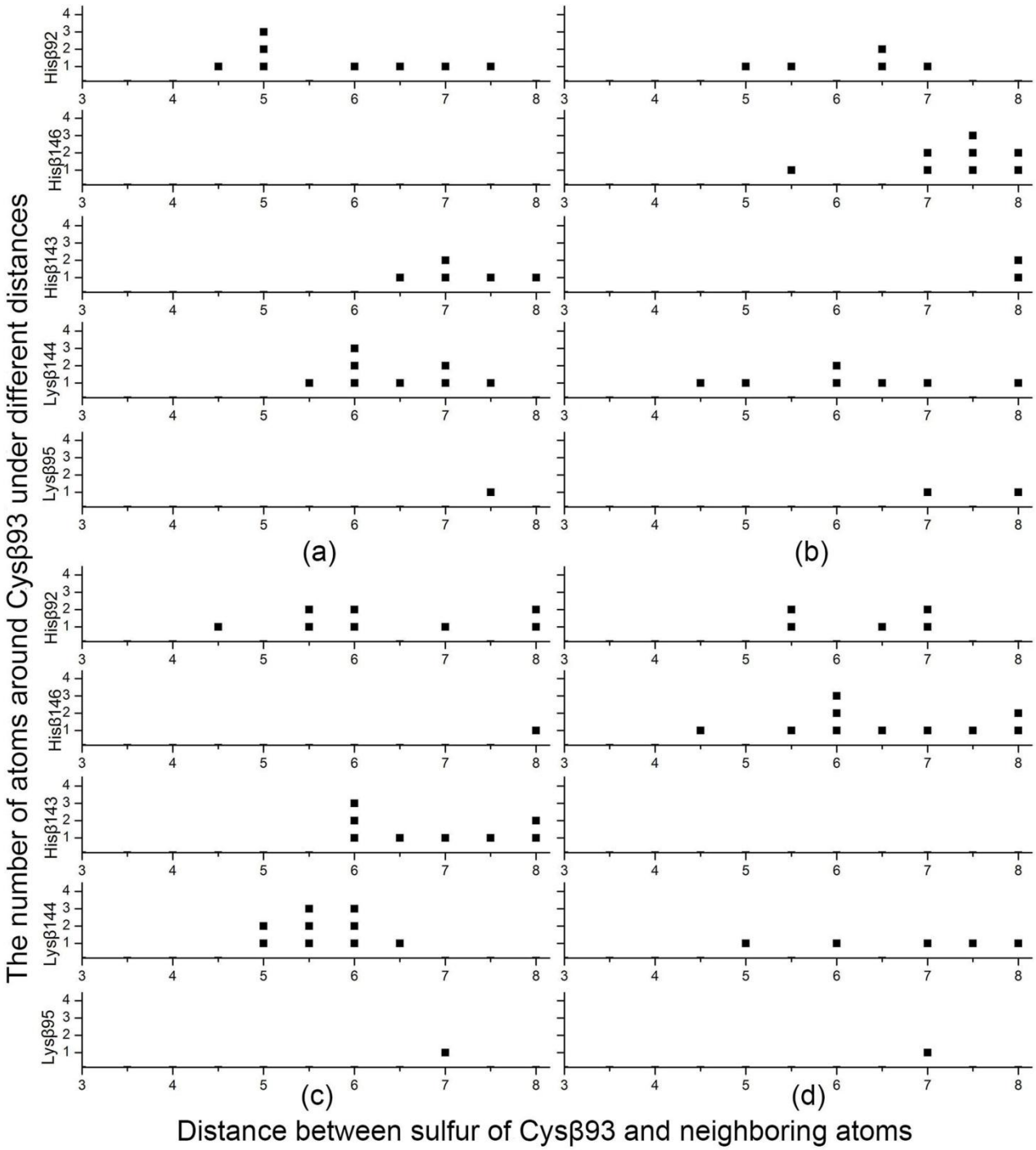

Fig. 3 The neighboring basic residues around the Cysβ93 in R-state (a), T-state (b), dep-R-state (c) and dep-T-state (d) hemoglobin. The x-axis represents the distance between the sulfur of the Cysβ93 and the neighboring atoms from different residues. The y-axis (■) represents the number of atoms.

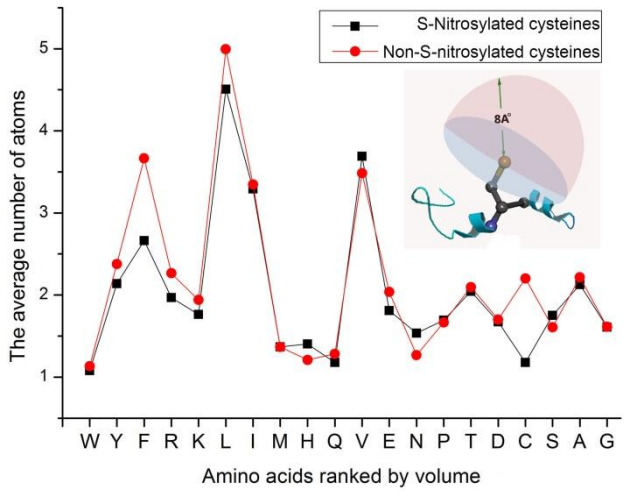

Fig. 4 Steric hindrance caused by the atoms in the half ball of 8 Å. The x-axis represents the different types of amino acids ranked by volume (BIGC670101 in AAindex) from large to small. The y-axis represents the average number of atoms in S-nitrosylated cysteine sites and non-S-nitrosylated cysteine sites.

Cite this: DOI: 10.1039/c0xx00000x

www.rsc.org/xxxxxx

ARTICLE TYPE

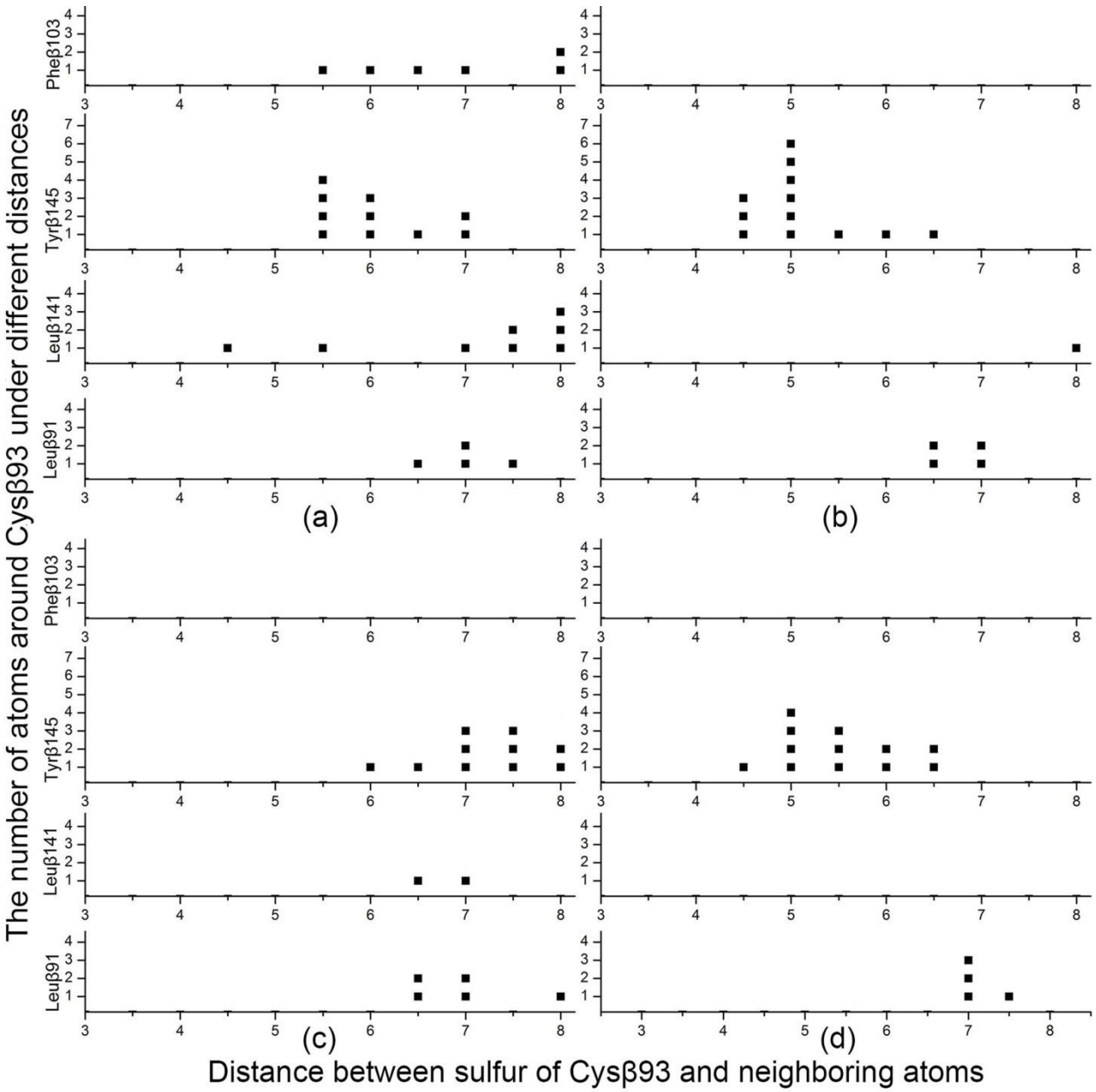

Fig. 5 The neighboring big-volume residues around the Cysβ93 in R-state (a), T-state (b), dep-R-state (c) and dep-T-state (d) hemoglobin. The x-axis represents the distance between sulfur of the Cysβ93 and the neighboring atoms from different residues. The y-axis (■) represents the number of atoms.

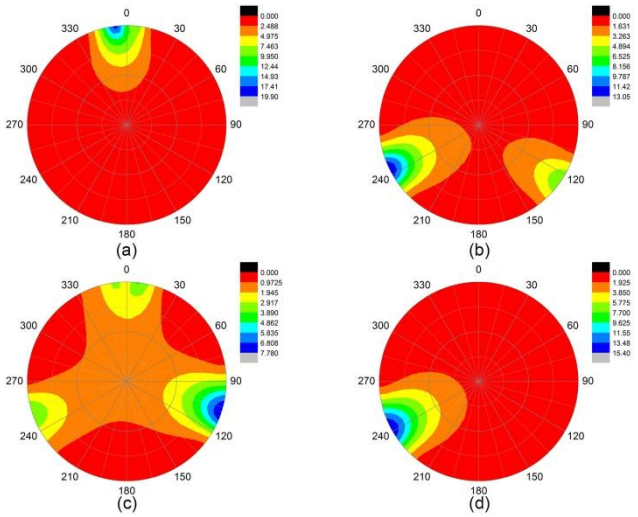

Fig. 6 The dihedral angle of Cysβ93 in R-state (a), T-state (b), dep-R-state (c) and dep-T-state (d) hemoglobin. The dihedral angle was analysed from 0 to 360˚. The colour bar represents the frequency (%) of the dihedral angle.

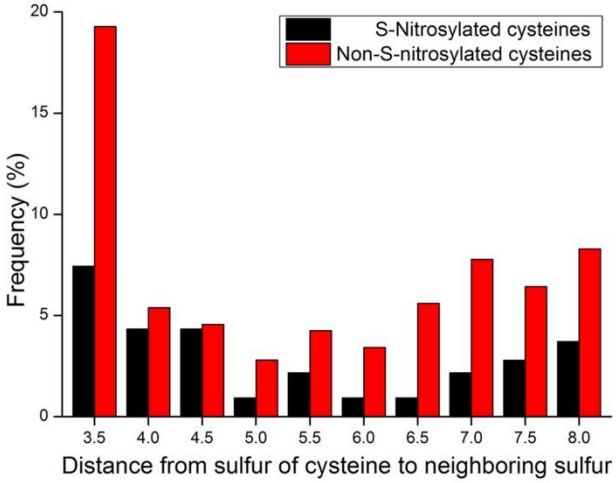

Fig. 7 The atomic distribution of the sulfur atoms of neighboring cysteines in S-nitrosylated and non-S-nitrosylated cysteine sets. The x-axis represents the distance from the sulfur of S-nitrosylated or non-S-nitrosylated cysteines to the sulfur of neighboring cysteines. The y-axis represents the frequency of neighboring sulfur atoms, which was normalized by the number of S-nitrosylated cysteines and the number of non-S-nitrosylated cysteines, respectively.

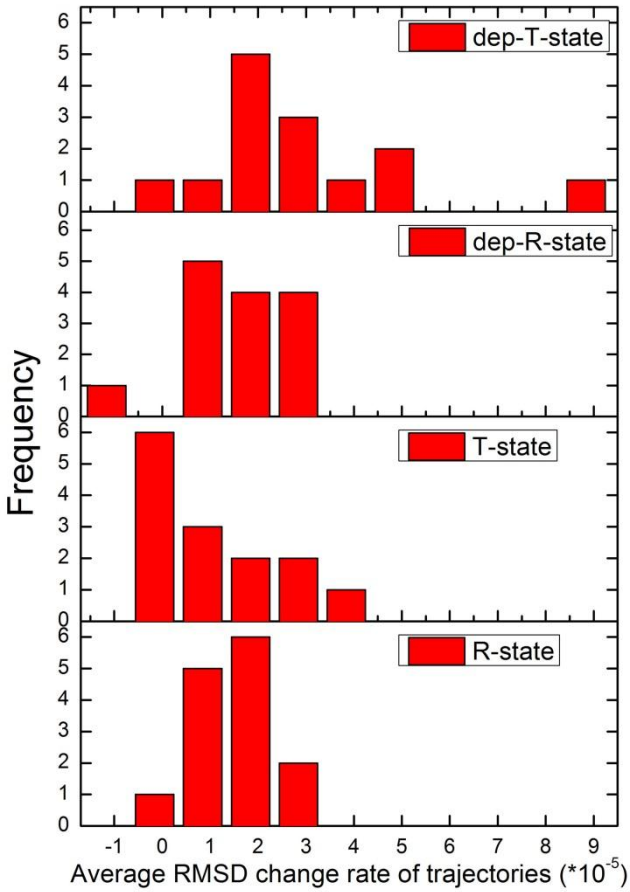

Fig. 8 The rate of change for RMSDs of the R-state, T-state, dep-R-state and dep-T-state hemoglobin in the repeated MD simulations. The x-axis represents the average rate of change calculated by RMSD curve in MD simulations. The y-axis represents the frequency of different rate of change.

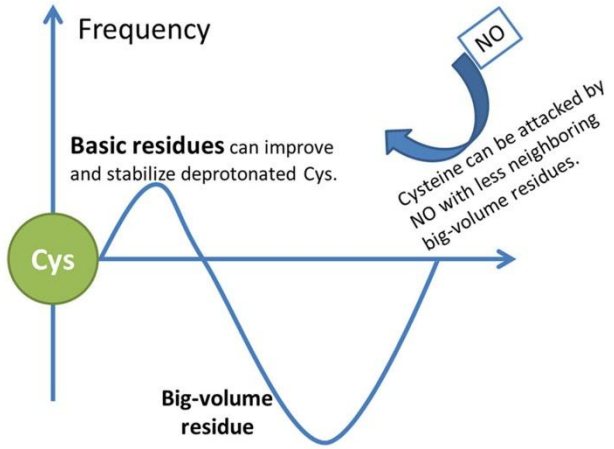

Fig. 9 The 3-D structural model of S-nitrosylation. The x-axis represents the distance to the sulfur of cysteine (green ball). The y-axis represents the frequency of the neighboring residues.

5

Table 1 The RMSF of the cysteines in the R-state and T-state hemoglobin. The Cysβ93 in the R-state can be S-nitrosylated. The cysteines in the T-state, as well as the Cysα104 and Cysβ112 in the R-state, cannot be S-nitrosylated.

	R-state (Å)	T-state (Å)
Cysα104	0.445	0.455
Cysβ93	**0.995**	0.755
Cysβ112	0.464	0.448

$$\text{Percentage difference value} = \frac{\text{PN(i)} - \text{NN(i)} \times \frac{\text{P}}{\text{N}}}{\text{P}} \times 100\% \quad (1)$$